31st Annual International Conference of the IEEE EMBS
Minneapolis, Minnesota, USA, September 2-6, 2009

Vibro-acoustography Imaging Applications for the Prostate

Mostafa Fatemi, *Senior Member, IEEE,* Farid G. Mitri, *Member, IEEE*

***Abstract*—Vibro-acoustography (VA) is a novel modality that has shown significant features in imaging hard inclusions and inhomogeneities within biological tissue. Here we focus on its applications for prostate imaging as well as some of its related feasibility studies to guide minimally-invasive therapies such as brachytherapy and cryosurgery.**

I. Introduction

PROSTATE cancer is recognized as one of the most prevalent malignant diseases and is the most commonly diagnosed cancer among men in the U.S. In 2008, an estimated 186 320 men will be diagnosed with prostate cancer and 28 660 men will die of this disease [1]. Quantitative screening for prostate cancer at the early stage will reduce the mortality number, and allows efficient minimally invasive therapies such as brachytherapy, thermo-ablation or cryosurgery to be undertaken.

Conventional transrectal ultrasound (TRUS) is regularly used for prostate diagnostic imaging, brachytherapy seed implantation monitoring [2], and monitoring prostate cryotherapy [3, 4]. However, there are some major limitations with TRUS. Namely, ultrasound imaging inherently suffers from speckle. Speckle is the snowy pattern that is caused by the interference of energy from randomly distributed scatterers too small to be resolved by the imaging system, it degrades both the spatial and contrast resolution and thereby reduces the diagnostic value of the images. Thus, many lesions in tissue go undetected. Furthermore, speckle masks small details in tissue. Furthermore, in the American Cancer Society prostate screening study of 2427 men, a total of 56 cancers were detected [5]. Of these, TRUS detected 43 (77%), indicating the limited sensitivity of the technique. In addition, TRUS has particularly low specificity; in this same study, 330 of the 2427 men had a suspicious ultrasound, but only 56 of these men had prostate cancer. TRUS has also been used for local staging of prostate cancer. Sonographic signs of T3 disease include bulging or irregularity of the prostate margin, asymmetry of the seminal vesicles, and obliteration of the ejaculatory duct or the fat plane between the seminal vesicles and the prostate [6, 7]. However, despite initial enthusiasm, the results have not been satisfactory. In a multi-institutional prospective study, TRUS was no better than DRE in local staging [6, 7]. Consequently, there is a need for improved means of imaging in detecting prostate cancer.

Manuscript received April 23, 2009. This work was supported in part by the National Institute of Health under Grant CA 91956–06P2.

F. G. Mitri and M. Fatemi are with the Department of Physiology and Biomedical Engineering, Mayo Clinic College of Medicine, Rochester, MN 55905 USA (e-mail: mitri.farid@mayo.edu; fatemi@mayo.edu).

Moreover, common treatments for early stage prostate cancer include radical prostatectomy, external beam radiation therapy (EBRT), radioactive brachytherapy seed implantation, cryosurgery and thermal ablation. Although there remains controversy regarding many aspects of treatment for such patients [8], permanent prostate brachytherapy (PPB) remains the most frequently practiced form of minimally invasive treatment for prostate cancer. Nonetheless, improved methods of image guidance are needed for PPB and are under active investigation [9-11]. A current limitation with PPB is the need for intraoperative real-time dosimetry [12, 13]. In this attempt, it is essential to identify all implanted seeds; the accuracy of seed placement and, consequently, the ability to immediately image and monitor their placement relative to prostate anatomy is a critical determinant of outcome.

Currently, the common imaging modalities used for seed placement, TRUS and fluoroscopy, do not routinely provide enough information to allow 'real-time' intraoperative dosimetry. Nevertheless, investigations involving TRUS-fluoroscopic image fusion are underway which are designed to address this problem [14, 15]. There remain however potential limitations of the image fusion approach provided as discussed in [15]. These limitations include those associated with decrease in accuracy in the seed localization process related to the use of multi-angle fluoroscopic projections [16] decrement in resolution associated with the image-fusion process [17, 18], and additional radiation exposure related to the use of fluoroscopy [19]. MR guided [10] and CT guided [11] PPB are other approaches which show promise for immediate radiation dosimetry, but equipment costs and logistical constraints in the hospital setting limit these methods in comparison to a purely ultrasound-based setting.

In addition, other minimally-invasive image guided therapies for prostate cancer will benefit from improved imaging. In cryotherapy ablation, zones of freezing are formed which produce near complete shadowing distal to the transducer on ultrasound examination [20]. No means are available in real-time to verify which areas of the prostate have experienced complete tissue freezing and ablation other than point measurement of temperature. The elastic properties of the frozen tissue change during freezing and after thawing. Therefore, it may be useful to monitor where freezing has occurred during the cryotherapy procedure.

All these limitations have provided the impetus to go beyond the common imaging tools for prostate imaging, and develop an imaging method that is: (a) noninvasive, (b) speckle free, (c) sensitive to tissue stiffness, (d) intra-operative, (e) capable of imaging brachytherapy seeds at any

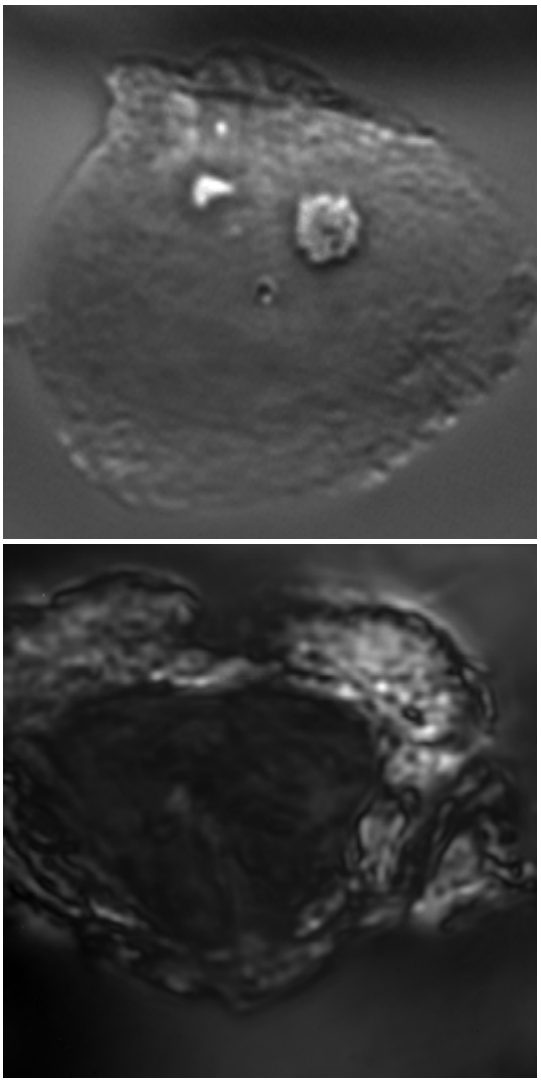

Fig. 1. VA images at Δf = 50 kHz for 2 prostates. The VA images show the prostatic tissue and borders, the urethra, and the surrounding tissue with remarkable detail. It is interesting to note the contrast and texture difference between the central and peripheral zones in the VA images, indicating the potential of VA in differentiating tissues with different biological structures. A few calcifications can also be seen in the image as bright spots.

orientation and (f) monitoring other minimally-invasive therapies. VA is an imaging method that we have recently developed in our lab [21-23] that offers all the qualities listed above. We have conducted prior studies on various aspects of VA imaging, including *in vitro* studies on tissue samples with different types of lesions to establish the applicability of imaging various organs, *in vivo* studies on human and animal subjects, and studies to develop the transducer array configuration for VA beam-forming [24-35]. The purpose of this paper is to provide an overview of what VA has yet accomplished in prostate imaging and guiding minimally invasive therapies.

II. VA IMAGING APPLICATIONS IN PROSTATE

A. Prostate Imaging

To date, we have performed a large number of VA imaging on excised human prostates. In this example we shall show two images of normal human prostates. The samples were fixed in formaldehyde and then embedded in gels. Each gel block including the prostate was scanned by VA separately. A confocal transducer at 3 MHz with a difference frequency of Δf = 50 kHz was used. The focal length and aperture size of the confocal transducer were 7 cm and 4.5 cm, respectively. The VA images show the prostatic tissue, its border, the urethra, and the surrounding tissue with remarkable detail. It is interesting to note the contrast and texture difference between the central and peripheral zones in the VA images, indicating the potential of VA in differentiating tissues with different biological structures. A few calcifications can also be seen in the image. Similarly, the resulting VA image showed the prostate, border, the urethra, and the surrounding tissue with remarkable detail. These preliminary results demonstrate the capability of VA in providing a clear image of the prostate.

B. Brachytherapy Seed Imaging

An experiment was conducted to investigate the performance of VA in imaging brachytherapy seeds in the prostate [30, 32]. A fresh cadaver prostate was implanted with a total of 22 seeds (11 standard and 11 corrugated (Echo) seeds from Amersham Inc.), and then the prostate was removed via conventional radical retropubic prostatectomy as performed by a urologic surgeon. Seventeen seeds remained in the prostate following prostatectomy as determined by fluoroscopic imaging. The *ex-vivo* cadaver prostate was then cast in formalin-catalyzed porcine gelatin (Type A, 300 bloom, Sigma G2500) at 15% concentration by volume to hold it in place. The gland was centered in the gelatin block, having approximately 1.6 cm of gelatin surrounding it on all sides and then immersed in a tank of degassed water. Twenty-four VA images at different depths were acquired by scanning the transducer over the gland surface by a 1 mm incremental step for a total depth of 24 mm deep inside the prostate gland. The images covered an area of 50 mm by 50 mm, scanned at 0.5 mm/pixel incremental step. For a better analysis of the results, the magnitude VA image taken at 1 mm deep from the surface of the prostate gland is displayed in Fig. 2 as an example. This image shows some of the seeds at various angles. Other seeds were visible when the scan was performed at different depths (not shown here). As the scan was performed in depth to cover the entire volume of the prostate, some of the seeds start to disappear from the VA image as they fall out of the focal region of the confocal transducer. After analyzing qualitatively the whole set of magnitude and phase VA images (not shown here), 12 seeds were detected out of 17 (71%) seeds implanted *in vitro*. This preliminary result (detection rate of 71%) has already surpassed the seed detection rate typically reported for conventional TRUS, to

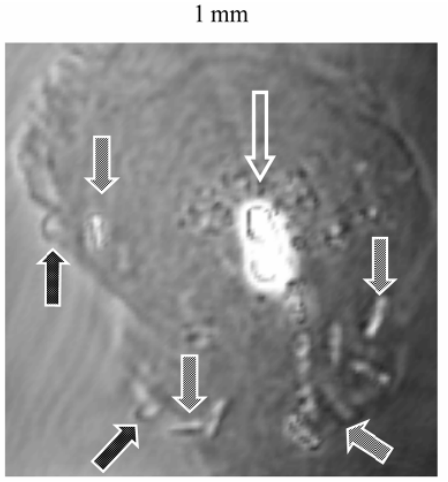

Fig. 2. Experimental magnitude VA image of the excised prostate showing seed location for 1 mm deep from the surface of the prostate gland. The image covered an area of 50 mm by 50 mm. This VA image shows some of the seeds (pointed by striped arrows) at various angles and other seeds appeared more clearly at different depths. One notices also that the intra-prostatic calcifications (pointed by an empty arrow) developed near the center of the gland reflect ultrasound waves and thus obscure some of the seeds. The dotted black arrows point to gas bubbles that were developed at the prostatic tissue-gelatin interface after embedding the prostate in the gel phantom.

be approximately 30%-50% [36]. The reason for missing some of the seeds is the unusually large calcification at the center that blocked the ultrasound from reaching the seeds behind it. If we exclude those seeds hidden by the calcification from our calculations, then the seed detection rate by VA may approaches 100%. This promising result encourages us to further develop and optimize VA to achieve an even higher seed detection rate.

C. *Imaging Cryotherapy Frozen Tissue*

To demonstrate the potential of VA in imaging frozen tissue regions, a freshly excised human prostate was removed via conventional radical retropubic prostatectomy as performed by a urologic surgeon. The excised human prostate was initially placed in a saline solution bag and baseline scans performed within two hours after excision. Reference images of the fresh unfrozen prostate specimen were obtained with the VA system apparatus [31]. A mixture of alcohol with dry ice was use to freeze a portion of the specimen down to -35°C as measured by a microcomputer thermometer (Omega Engineering, Model HH-72 T, Stanford CT, USA). The partially frozen prostate was subsequently placed within the water tank 27°C and VA images were acquired at 4, 10, 16, 60 and 120 minute intervals as the frozen portion of the prostate thawed. The images were acquired by scanning the transducer over the gland surface while recording the resulting acoustic emission pressure field. The images covered an area of 80 mm by 60 mm, scanned at 0.5 mm/pixel incremental steps. Fig. 3 shows seven VA images at different time intervals; prior to freezing (Fig. 3-(a)); immediately after freezing (Fig. 3-(b)); 4 minutes after freezing (Fig. 3-(c)); and 120 minutes after freezing so the prostate was completely

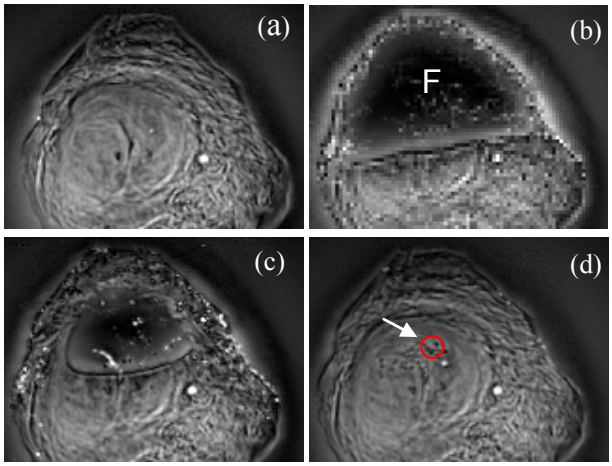

Fig. 3. VA images of intact (a), frozen (b and c), and thawed (d) excised prostate specimen. The frozen region is a solid dark region indicated by "F". (a) is prior to freezing, (b) is immediately after freezing, (c) is 4 minutes after freezing, and (d) is after 120 minutes when the prostate was completely thawed. There are some changes in the prostate texture in the previously frozen part, indicated by the arrow, and the top portion of the prostate is darker in (d) than in (a). The arrow in (d) points to the urethra that is surrounded by a red circle.

thawed (Fig. 3-(d)). The VA image obtained prior to freezing shows the prostate texture as well as two bright dots which correspond to intraprostatic calcifications. Immediately after freezing, the prostate frozen part shows a dark region with a well-defined "rim" at the edge. More notably, after the tissue thaws, the previously frozen region shows coarser texture and still appears darker in the image than it appeared prior to freezing. Intraprostatic calcifications reappear in the image in addition to small icy "islands" shown as bright spots. As the frozen tissue continues thawing, the cryolesions showed markedly decreased contrast compared with normal unfrozen prostate. At the end of the freezing process, the small icy "islands" completely disappear and the bright spots show the intraprostatic calcifications.

III. Conclusion

A few representative examples on prostate imaging using VA were shown. VA provided unique information on a number of prostates that may be proven critical in accurate detection and characterization of normal and pathological tissues. In addition VA has shown significant capabilities in detecting PPB brachytherapy seeds and imaging prostate frozen parts *in vitro*. A challenge in VA imaging is the scanning mechanism that is a relatively lengthy process (~ 4 min to achieve a scan). A long imaging time is not desirable for prostate imaging because body motions within this period can introduce "motion artifact" in the images and the procedure anesthesia time could be impractical. Besides, proper monitoring of minimally-invasive therapies requires faster (real-time) imaging. Current research in our group is directed toward the development and testing of a linear array probe with dynamic focusing whereby the imaging time should be significantly reduced. Together with the advent of fast scanning and fast acquisition hardware/software, the VA

technique may find a wide variety of clinical applications.

ACKNOWLEDGMENT

We thank Pr. James F. Greenleaf, Dr. Azra Alizad, Dr. Brian J. Davis, and Randall R. Kinnick for their input and contributions.

REFERENCES

[1] A. Jemal, R. Siegel, E. Ward, Y. Hao, J. Xu, T. Murray, and M. J. Thun, "Cancer Statistics, 2008," *CA Cancer J Clin*, vol. 58, no. 2, pp. 71-96, 2008.

[2] H. H. Holm, N. Juul, J. F. Pedersen, H. Hansen, and I. Stroyer, "Transperineal 125iodine seed implantation in prostatic cancer guided by transrectal ultrasonography," *The Journal Of Urology*, vol. 130, no. 2, pp. 283-286, 1983.

[3] G. Onik, C. Cobb, J. Cohen, J. Zabkar, and B. Porterfiled, "US Characteristics of Frozen Prostate," *Radiology*, vol. 168, pp. 629-631, 1988.

[4] G. Onik, "Image-Guided Prostate Cryosurgery: State of the Art," *Cancer Control*, vol. 8, no. 6, pp. 522-531, 2001.

[5] C. Mettlin, "Preliminary findings from the American Cancer Society National Prostate Cancer Detection Project.," presented at 5th International Syposium on Transrectal Ultrasound in the Diagnosis and Management of Prostate Cancer, Chicago, IL, 1990.

[6] J. Smith, Jr., "Transrectal ultrasonography for the detection and staging of carcinoma of the prostate," *Journal of Clinical Ultrasound*, vol. 24, no. 8, pp. 455-461, 1996.

[7] J. Smith, P. Scardino, M. Resnick, A. Hernandez, S. Rose, and M. Egger, "Transrectal ultrasound versus digital rectal examination for the staging of carcinoma of the prostate: Results of prospective multi-institutional trial," *Journal of Urology*, vol. 157, pp. 902-906, 1997.

[8] F. Fowler, Jr, M. McNaughton Collins, P. Albertson, A. Zietman, D. Elliott, and M. Barry, "Comparison of recommendations by urologists and radiation oncologists for treatment of clinically localized prostate cancer.," *Journal of the American Medical Association*, vol. 283, no. 24, pp. 3217-3222, 2000.

[9] Y. Yu, L. Anderson, Z. Li, D. Mellenberg, R. Nath, M. Schell, F. Waterman, A. Wu, and J. Blasko, "Permanent prostate seed implant brachytherapy: Report of the American Association of Physicists in Medicine Task Group No. 64," *Medical Physics*, vol. 26, no. 10, pp. 2054-2076, 1999.

[10] A. D'Amico, "Real-time magnetic resonance image-guided interstitial brachytherapy in the treatment of select patients with clinically localized prostate cancer.," *International Journal of Radiation Oncology Biology Physics*, vol. 42, no. 3, pp. 507-515, 1998.

[11] P. Koutrouvelis, "Three-dimensional stereotactic posterior ischiorectal space computerized tomography guided brachytherapy of prostate cancer: A preliminary report," *Journal of Urology*, vol. 159, no. 1, pp. 142-145, 1998.

[12] S. J. Hsu, B. J. Fahey, D. M. Dumont, P. D. Wolf, and G. E. Trahey, "Challenges and implementation of radiation-force imaging with an intracardiac ultrasound transducer," *IEEE Transactions on Ultrasonics, Ferroelectrics, and Frequency Control*, vol. 54, no. 5, pp. 996-1009, 2007.

[13] D. I. Holmes, B. Davis, and R. Robb, "3D localization of implanted radioactive sources in the prostate using trans-urethral ultrasound," *Studies in Health Technology & Informatics*, vol. 81, pp. 199-205, 2001.

[14] S. Narayanan, P. Cho, and R. Marks, II, "Fast cross-projection algorithm for reconstruction of seeds in prostate brachytherapy," *Medical Physics*, vol. 29, pp. 1572-1579, 2002.

[15] Y. Su, B. Davis, M. Herman, W. LaJoie, and R. Robb, "Brachytherapy seed localization from fluoroscopic images using a statistical classifier.," *Proceedings of the Sixth Annual Conference on Medical Image Computing & Computer Assisted Intervention*, vol. 2879, pp. 945-946, 2003.

[16] Y. Su, B. Davis, M. Herman, and R. Robb, "Prostate brachytherapy seed localization by analysis of multiple projections: identifying and addressing the seed overlap problem," *Medical Physics*, vol. 31, no. 5, pp. 1277-87, 2004.

[17] J. Fitzpatrick, J. West, and C. Maurer, Jr, "Predicting error in rigid-body point-based registration.," *IEEE Transactions on Medical Imaging*, vol. 17, no. 5, pp. 694-702, 1998.

[18] Y. Su, B. Davis, M. Herman, and R. Robb, "Fluoroscopy to ultrasound image registration using implanted seeds as fiducials during permanent prostate brachytherapy," *Proceedings of Medical Imaging 2004: Visualization, Image-Guided Procedures, and Display*, vol. 5367, pp. 371-378, 2004.

[19] D. Schwartz, B. Davis, R. Vetter, T. Pisansky, M. Herman, T. Wilson, W. LaJoie, and A. Oberg, "Radiation exposure to operating room personnel during transperineal interstitial permanent prostate brachytherapy.," *Brachytherapy*, vol. 2, no. 2, pp. 98-102, 2003.

[20] B. Han, K. Wallner, G. Merrick, W. Butler, S. Sutlief, and J. Sylvester, "Prostate brachytherapy seed identification on post-implant TRUS images," *Medical Physics*, vol. 30, pp. 898-900, 2003.

[21] M. Fatemi and J. Greenleaf, "Ultrasound stimulated vibro-acoustic spectroscopy," *Science*, vol. 280, pp. 82-85, 1998.

[22] M. Fatemi and J. Greenleaf, "Vibro-acoustography: an imaging modality based on ultrasound stimulated acoustic emission," *Proceedings of the National Academy of Sciences USA*, vol. 96, pp. 6603-6608, 1999.

[23] M. Fatemi, A. Manduca, and J. Greenleaf, "Imaging elastic properties of biological tissues by low-frequency harmonic vibration," *Proceedings of the IEEE*, vol. 91, no. 10, pp. 1503-1517, 2003.

[24] A. Alizad, L. E. Wold, J. F. Greenleaf, and M. Fatemi, "Imaging mass lesions by vibro-acoustography: Modeling and experiments," *IEEE Transactions on Medical Imaging*, vol. 23, no. 9, pp. 1087-1093, 2004.

[25] A. Alizad, M. Fatemi, L. E. Wold, and J. F. Greenleaf, "Performance of vibro-acoustography in detecting microcalcifications in excised human breast tissue: A study of 74 tissue samples," *IEEE Transactions on Medical Imaging*, vol. 23, no. 3, pp. 307-312, 2004.

[26] M. Fatemi, L. E. Wold, A. Alizad, and J. F. Greenleaf, "Vibro-acoustic tissue mammography," *IEEE Transactions on Medical Imaging*, vol. 21, no. 1, pp. 1-8, 2002.

[27] J. F. Greenleaf, M. Fatemi, and M. F. Insana, "Selected methods for imaging elastic properties of biological tissues," *Annual Review of Biomedical Engineering*, vol. 5, pp. 57-78, 2003.

[28] F. G. Mitri, P. Trompette, and J. Y. Chapelon, "Improving the use of vibro-acoustography for brachytherapy metal seed imaging: A feasibility study," *IEEE Transactions on Medical Imaging*, vol. 23, no. 1, pp. 1-6, 2004.

[29] F. G. Mitri, J. F. Greenleaf, and M. Fatemi, "Chirp imaging vibro-acoustography for removing the ultrasound standing wave artifact," *IEEE Transactions on Medical Imaging*, vol. 24, no. 10, pp. 1249-1255, 2005.

[30] F. G. Mitri, B. J. Davis, J. F. Greenleaf, and M. Fatemi, "In vitro comparative study of vibro-acoustography versus pulse-echo ultrasound in imaging permanent prostate brachytherapy seeds," *Ultrasonics*, vol. 49, no. 1, pp. 31-38, 2009.

[31] F. G. Mitri, B. J. Davis, A. Alizad, J. F. Greenleaf, T. M. Wilson, L. A. Mynderse, and M. Fatemi, "Prostate Cryotherapy Monitoring Using Vibroacoustography: Preliminary Results of an Ex Vivo Study and Technical Feasibility," *IEEE Transactions on Biomedical Engineering*, vol. 55, no. 11, pp. 2584-2592, 2008.

[32] F. G. Mitri, B. J. Davis, M. W. Urban, A. Alizad, J. F. Greenleaf, G. H. Lischer, T. M. Wilson, and M. Fatemi, "Vibro-acoustography Imaging of Permanent Prostate Brachytherapy seeds in an excised human prostate - Preliminary Results and Technical Feasibility," *Ultrasonics*, vol. 49, no. 3, pp. 389-394, 2009.

[33] C. Pislaru, B. Kantor, R. R. Kinnick, J. L. Anderson, M. C. Aubry, M. W. Urban, M. Fatemi, and J. F. Greenleaf, "In vivo vibroacoustography of large peripheral arteries," *Investigative Radiology*, vol. 43, no. 4, pp. 243-252, 2008.

[34] G. T. Silva, J. F. Greenleaf, and M. Fatemi, "Linear arrays for vibro-acoustography: A numerical simulation study," *Ultrasonic Imaging*, vol. 26, no. 1, pp. 1-17, 2004.

[35] G. T. Silva, S. G. Chen, A. C. Frery, J. F. Greenleaf, and M. Fatemi, "Stress field forming of sector array transducers for vibro-acoustography," *IEEE Transactions on Ultrasonics Ferroelectrics and Frequency Control*, vol. 52, no. 11, pp. 1943-1951, 2005.

[36] Y. Su, B. J. Davis, M. G. Herman, A. Manduca, and R. A. Robb,

"Examination of dosimetry accuracy as a function of seed detection rate in permanent prostate brachytherapy," *Medical Physics*, vol. 32, no. 9, pp. 3049-3056, 2005.